IEEE Access
Multidisciplinary ⋮ Rapid Review ⋮ Open Access Journal

Received January 6, 2020, accepted January 17, 2020, date of publication January 21, 2020, date of current version January 30, 2020.

Digital Object Identifier 10.1109/ACCESS.2020.2968341

Design of a Planar Transmission Line Balun Based on Novel Phase Inverter

YA-QING YU[1], WEN JIANG[1], (Member, IEEE), LV QIN[2], HAO-YU SHAO[1], AND SHU-XI GONG[1], (Member, IEEE)

[1]National Key Laboratory of Antennas and Microwave Technology, Xidian University, Xi'an 710071, China
[2]Research and Development Center, the 39th Research Institute of China Electronics Technology Group Corporation, Xi'an 710071, China

Corresponding author: Wen Jiang (jw13@vip.qq.com)

This work was supported by the National Basic Research Program of China-973 Program under Grant 2015CB857100.

ABSTRACT In this paper, a planar ultrawideband (UWB) transmission line balun based on a novel phase inverter is proposed, which consists of three coaxial connector to double-sided parallel-strip line (DSPSL) transitions, a two-section Wilkinson divider, and a phase inverter. In the phase inverter, a 90-degree rotating transition is applied to realize field inversion. It maintains good structural uniformity of the two outputs of the balun and ensures the characteristics of equal energy division and a stable 180-degree phase difference in wide frequency band. Compared with other designs, the proposed balun has the advantages of easy to design, UWB operation, low reflection, equal power division and a stable phase difference. The presented balun works in the 0.52 GHz to 2.32 GHz band, covering 4.46 octaves. The measurements can achieve the reflection, amplitude imbalance and phase imbalance characteristics below −15 dB, ±0.46 dB and ±4 deg, respectively. The designs including the phase inverter and balun are fabricated and measured to verify the performance, and the measurements are found to be in good agreement with the simulations. In addition, the UWB potential of the porposed balun is studied. From an example based on a 1:2 balun, we can conclude that the proposed balun has the potential to work in a wider frequency band within the range of 0.1 GHz to 3GHz.

INDEX TERMS Double-sided parallel-strip line (DSPSL), phase inverter, transmission line balun, ultrawideband (UWB).

I. INTRODUCTION

The balun is a transformer used to connect balanced circuits to unbalanced ones. Wideband baluns are widely used in push–pull amplifiers, double balanced mixers, differentially fed antennas, and other balanced-to-unbalanced conversion circuits. Therefore, it is of great significance to design a balun which is easy to design, ultra wideband (UWB) operation and high performance.

The common forms of the balun are Marchand balun, coupled-line balun, microstrip line (MSL) to balanced double-sided parallel strip line (DSPSL) balun, and transmission line balun. The Marchand balun has the advantages of flexible design and compact size, which is often used in the broadband power amplifiers [1], double-balanced mixers [2], tightly coupled dipole antennas [3], and other integrated designs [4]. However, Marchand balun has a high design complexity, as the tight coupling factor needs to be calculated. The coupled-line balun has a simple structure without via holes [5], [6], but it needs a thick substrate with a low dielectric constant, and a long and narrow coupling structure to achieve a high even mode impedance, which results in high insertion loss and large device size [7]. The MSL to DSPSL balun has an ultrawide working bandwidth and is easy to fabricate, which is widely used in the feed of the spiral antennas [8] and push-pull power amplifiers [9], but it suffers a poor match and phase fluctuation problem. Other baluns based on the four-port passive circuit, such as rat-race hybrids [10] and magic tees [11], [12], all have the shortcoming of a narrow bandwidth. The newly emerging filtering balun based on the forms above can simultaneously achieve the function of a balun and a filter [13]–[16], with disadvantages that depend on the balun form adopted. However, none of the baluns reported above both have the advantages of easy to design, UWB operation and high performance.

A transmission line balun typically consists of two portions: the first portion divides the signal into two parts having an equal amplitude and phase, and the second portion ensures

The associate editor coordinating the review of this manuscript and approving it for publication was Yasar Amin.

that the two parts have a phase difference of 180 degrees. So, the performance of the transmission line balun is determined by the divider, the impedance transformer and the phase inverter. Since these three parts can be designed separately, the design difficulty of the whole balun can be reduced to some extent, and the design flexibility can be guaranteed. Therefore, the transmission line balun has the potential to meet our requirements.

Until now, much work has been done, in which the principles of power division and impedance transformation have a mature theoretical basis. Therefore, the main differences between each work can be concluded into the principle of phase inversion. A 90-degree phase shifter-based balun realized by a Lange coupler [17] or right/left artificial transmission line [18] can achieve a −10dB impedance bandwidth of 2.2 octaves and 2.42 octaves, respectively. This type of transmission line balun is complex in designing the 90-degree phase shifter. The ferrite-based balun has low-pass characteristics with good matching, stable amplitude and phase characteristics at low frequencies [19]. However, it is not easy to fabricate such a device due to its nonplanar structure; in addition, this design will suffer a high insertion loss in high-frequency band due to the large tangential loss angle of the magnetic material. Another type of phase inversion can be realized by opposite field propagation after through the coupling slot [20]–[22]. This kind of balun can ensure stable amplitude and phase characteristics for an UWB, but it suffers a radiation effect as the coupling slot need to work in a resonant state. The latter method of phase inversion lies on the conductor exchange of a DSPSL, which is most likely to meet our requirements. However, the performance will deteriorate if the conductors of the DSPSL are directly exchanged without any transitions [23]–[25].

In this work, a novel phase inverter with improvements on the last method mentioned above is introduced first. The phase inverter can be used to realize the out-of-phase characteristic of two outputs by field rotation. A 90-degree rotating transition is adopted, which plays a transitional role in the process of field rotation and provides the two outputs with good structural uniformity to ensure low amplitude and phase imbalance. Based on the phase inverter, a transmission line balun is proposed thereafter. It can be found that the balun have several attractive advantages, which are: 1) easy to design; 2) UWB operation; 3) small amplitude difference; 4) stable out-of-phase property; 5) perfect matching; 6) flexible design for different requirements of working band, reflection, isolation and so on.

The organization of this paper will be arranged as follows. In section II, the working principle and performance of the phase inverter are introduced first. Then, the composition, detailed design and performance of the balun are presented. In section III, the UWB potential of the balun is studied. Finally, section IV summarizes the content of the paper.

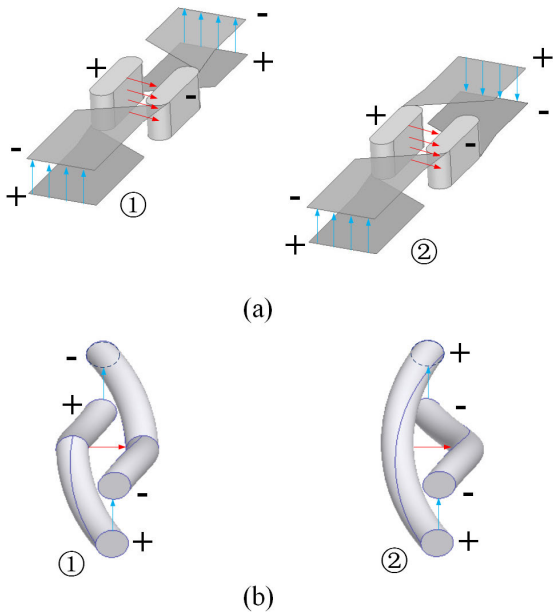

FIGURE 1. Structure and electric field vector distribution for the phase inverter. (a) Model. (b) Analogy diagram.

II. DESIGN OF THE BALUN

A. INTRODUCTION OF PHASE INVERTER

The structure and electric field vector distribution for the working phase inverter is depicted in Fig. 1. The idea arises from a pair of twisted parallel double transmission line with the same starts and reverse ends, as shown in Fig. 1(b). Since the characteristic impedance of the parallel double transmission line is mainly determined by the spacing and the dielectric constant, the impedance of the two lines in Fig. 1 can achieve nearly the same. In addition, their close electrical lengths also ensure the close phase shift characteristic. These two features above are particularly suitable for the transmission line balun with UWB operation, low amplitude and phase imbalance. To explain the process more clearly, the electric field vectors are marked in the form of arrows in Fig. 1, and a detailed explanation can be expressed as follows.

We assume that the initial electric field phases of the two ways' signals are the same. When these signals pass through the part composed of metallized slots, their electric field vectors rotate 90 degrees in space but still keep in-phase. However, as the signals keep propagating, the electric field vectors of the two branches rotate by 90 degrees in two opposite directions, resulting in the signal phases of the two branches being opposite to each other.

Compared with traditional structures, the proposed phase inverter has a 90-degree rotation transition structure, which can achieve a 180-degree phase difference between two balanced ports more smoothly. Due to the high similarity between two branches of the proposed inverter, the stabilities of the phase and amplitude imbalance are guaranteed, which will be verified in the next part.

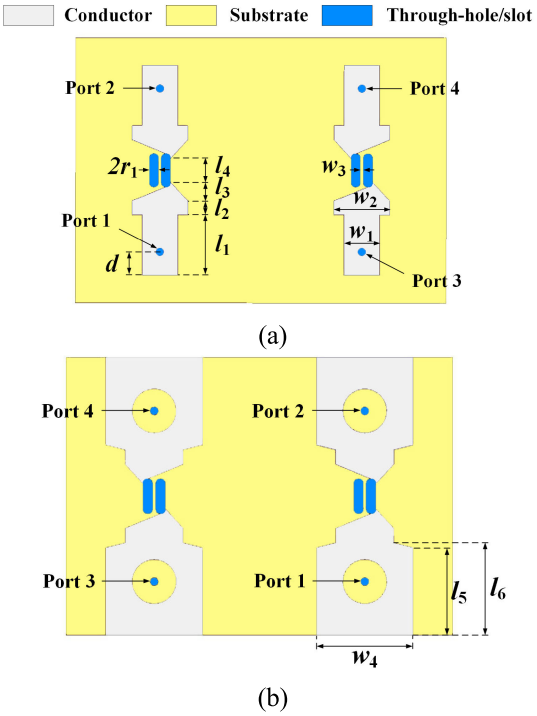

FIGURE 2. Structural configuration of the phase inverter. (a) Top view. (b) Bottom view.

B. PERFORMANCE VERIFICATION

To validate the performance of the proposed phase inverter, an example is presented, as depicted in Fig. 2. The phase inverter is composed of four coaxial connectors to DSPSL transitions, two DSPSLs, and two pairs of metalized through-slots. The coaxial connector to DSPSL transition can convert the TEM mode of coaxial cable to the TEM mode of DSPSL. In this example, the characteristic impedances of all parts are designed to 50 ohms to facilitate the measurement.

The main design parameters of the inverter are the widths of the 50-ohm DSPSL and the spacing of each pair of through-slots. As the electric field distribution of the DSPSL is similar to that of the MSL, the characteristic impedance of the DSPSL with a height of h is approximately twice that of an MSL with equal width and height of $h/2$ [26]. Therefore, when h in the formula of MSL [27] are replaced by $h/2$, the characteristic impedance of DSPSL should be $Z_{\mathrm{DSPSL}}(h) = 2Z_{\mathrm{MSL}}(h/2)$. The characteristic impedance of the DSPSL can be expressed as follows,

$$\begin{cases} Z_{\mathrm{DSPSL}} = \dfrac{120}{\sqrt{\varepsilon_{eff}}} \ln\left(\dfrac{4h}{w_{eff}} + \dfrac{0.5w_{eff}}{h}\right), & \dfrac{w}{h} \le 0.5 \\ Z_{\mathrm{DSPSL}} = \dfrac{240}{\sqrt{\varepsilon_{eff}}}\left[\dfrac{2w_{eff}}{h} + 1.393 \right. \\ \qquad \left. + 0.667 \ln\left(\dfrac{2w_{eff}}{h} + 1.444\right)\right]^{-1}, & \dfrac{w}{h} > 0.5 \end{cases} \tag{1}$$

$$\frac{w_{eff}}{h} = \frac{w}{h} \frac{2.5t}{\pi h}\left[1 + \ln\left(\frac{4\pi w}{t}\right)\right], \quad \frac{w}{h} \le \frac{1}{4\pi}, \tag{2}$$

$$\frac{w_{eff}}{h} = \frac{w}{h} + \frac{1.25t}{\pi h}\left[1 + \ln\left(\frac{h}{t}\right)\right], \quad \frac{w}{h} > \frac{1}{4\pi}, \tag{3}$$

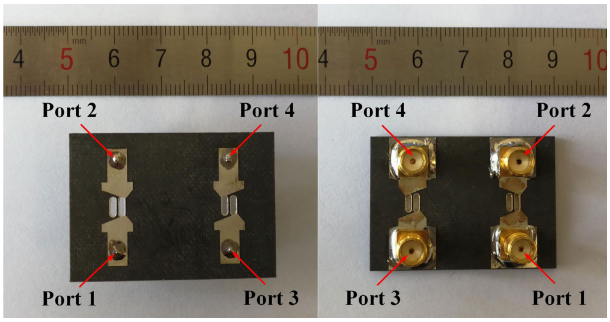

FIGURE 3. Fabrication of the phase inverter.

$$\varepsilon_{eff} = \frac{\varepsilon_r + 1}{2} + \frac{\varepsilon_r - 1}{2} \frac{1}{\sqrt{1 + \dfrac{6h}{w}}} - \frac{(\varepsilon_r - 1)t}{2.3h\sqrt{\dfrac{2w}{h}}}, \tag{4}$$

where w is the width of the strip line, h is the spacing of the two parallel-strip lines, t is the metal layer thickness of the strip line, and ε_r is the dielectric constant of the substrate.

With the help of (1) to (4) and MATLAB 2019a, the theoretical widths of the 50-ohm DSPSL can be determined to be approximately 6 mm for $t = 0.1$ mm. Considering that the phase inverter can be seen as a 90-degree rotating DSPSL with its width equal to the thickness of the substrate, its spacing for metallized through-slots can also be calculated to be approximately 0.42 mm.

To analyze the performance of the phase inverter, some simulations are carried out by the full-wave simulation software of ANSYS HFSS 2018, and a corresponding fabrication is manufactured with the etching technique, as shown in Fig. 3. In this design, an RT5880 substrate with a dielectric constant of 2.2 and thickness of 1.57 mm is adopted. The internal and external diameters of the coaxial structure are 0.84 mm and 4.56 mm, respectively. Other optimized parameters are (unit: mm): $d = 2.5, w_1 = 3.8, w_2 = 6, w_3 = 0.32, w_4 = 10, l_1 = 6.5, l_2 = 1.5, l_3 = 2, l_4 = 2.6, l_5 = 9, l_6 = 9.5, r_1 = 0.5$. The fabrication is measured by Rohde & Schwarz ZND vector network analyzer (VNA) with two coaxial cables in the form of two-port test. The comparison results obtained from measurements and simulations are depicted in Fig. 4.

From the results, we can see that in the 0.1-3 GHz band, the simulations of the part without phase inversion (port 1 to port 2) are in good agreement with the measurements. However, the simulations and measurements of another part with phase inversion (port 3 to port 4) do not coincide with each other across 0.1-0.4 GHz due to a strong resonance. As a result, in the band of 0.4 GHz to 3GHz, the proposed phase inverter can achieve the reflection, amplitude imbalance and phase imbalance characteristics below -10 dB, ± 0.4 dB and ± 4 deg, respectively.

Considering that the phase inverter is connected to the VNA by two coaxial cables during the test, we boldly speculate that the resonance is generated by the circuit formed with the phase inversion structure, two cables and VNA source.

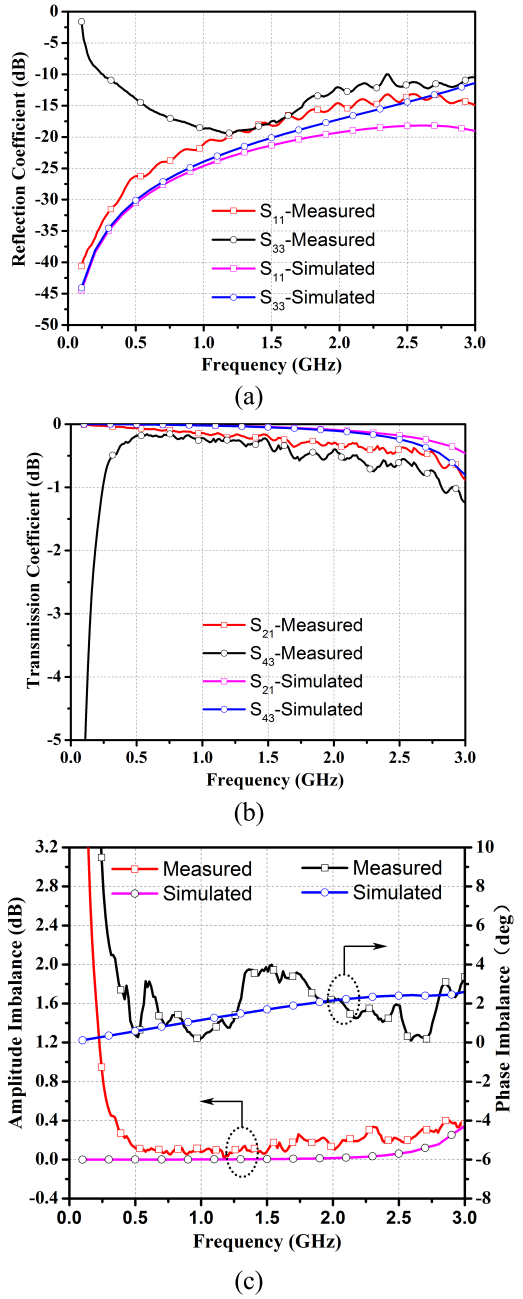

FIGURE 4. A Comparison between simulations and measurements of the phase inverter when two VNA cables are used in the test. (a) Reflection coefficient. (b) Transmission coefficients. (c) Amplitude imbalance and phase imbalance.

To verify this conjecture, the reflection coefficient characteristic for the phase inverter is retested when a matched load and one VNA cable are used to carry out the one-port test, as shown in Fig. 5.

As predicted, the resonance is removed by breaking the resonance circuit. Other differences between simulations and measurements are mainly attributed to the manufacture errors. For instance, the etching technique can achieve

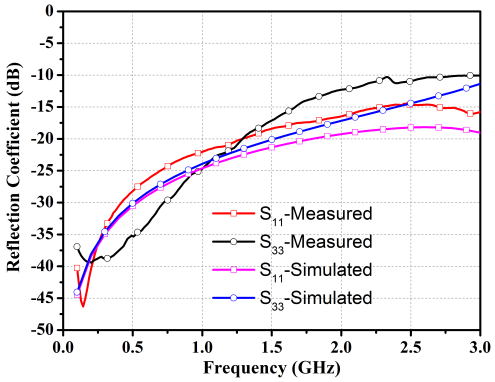

FIGURE 5. The reflection coefficients for port 1 and port 3 when matching load and one cable of the VNA are used in measurement.

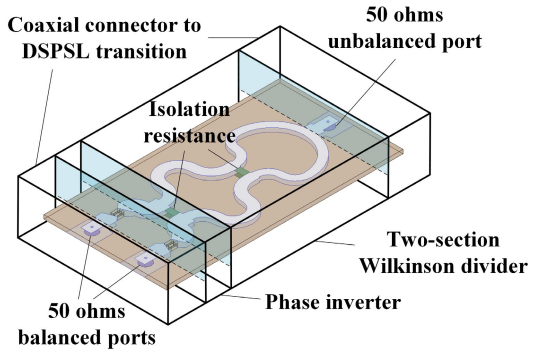

FIGURE 6. Configuration of the balun.

a processing accuracy of ±0.02 mm, but the positioning accuracy of the metallized through-slots and the surface metal thickness of the metallization slot can only be guaranteed within ±0.1 mm and ±0.075 mm, respectively. To simply calculate the impact of processing errors, we assume that the spacing of each pair of metallized slots varies in the range of 0.42 mm ±0.175 mm. Then, with the help of (1) to (4), we can theoretically figure out that the characteristic impedance of the phase inversion structure varies from approximately −35.65% to 30.76%.

Based on the novel phase inverter presented above, an UWB transmission line balun is designed thereafter.

C. STRUCTURAL DESIGN OF BALUN

As shown in Fig. 6, the proposed balun is composed of three coaxial connector to DSPSL transitions, a two-section Wilkinson divider, and a phase inverter. The two-section Wilkinson divider consists of a two-way power divider and a two-section Wilkinson quarter-wave impedance transformer, which divides the 50-ohm DSPSL into two 100-ohm DSPSLs via a T-junction, and then transforms the impedance of the two DSPSLs from 100 ohms back to 50 ohms. Because the two-section Wilkinson divider requires the two ends of isolation resistance in phase to achieve high isolation between two outputs, a strategy based on placing a divider before an inverter should be adopted.

TABLE 1. Parameters of the two-section Wilkinson transformer.

Section	Characteristic impedance (Ω)	Theoretical width of DSPSL (mm)	Isolation resistance (Ω)
1	81.99	3.12	98.01
2	60.985	4.68	241.02

The impedance and phase transformation strategy can be briefly expressed as follows: First, the 50-ohm coaxial cable is matched with the 50-ohm input of the two-section Wilkinson divider by the coaxial connector to DSPSL transition. Second, the two-section Wilkinson divider divides the 50-ohm DSPSL into two in-phase 50-ohm DSPSLs. Third, one of the in-phase 50-ohm DSPSLs realizes phase inversion, while the other remains unchanged when passing through the phase inverter. Finally, two out-of-phase 50-ohm DSPSLs are matched with two 50-ohm coaxial cables to output.

As is easy to know, the amplitude and phase imbalance of the balun are mainly restricted by the phase inverter, while the isolation and reflection characteristic are simultaneously determined by the phase inverter, the two-section Wilkinson divider and the coaxial connector to DSPSL transitions. Therefore, the two-section Wilkinson divider is designed next.

In the two-section Wilkinson divider, each length of the two-section quarter-wave impedance transformer is one fourth of the wavelength corresponding to the central frequency according to the working band. Considering the bandwidth limit of the transformer and phase inverter, the experimental band is set from 0.5 GHz to 2.5 GHz. Therefore, two quarter wavelengths can be calculated by using the equation of $L = c/(f_0\sqrt{\varepsilon_r}) \approx 40.4$ mm when the central frequency of 1.25 GHz is set. The isolation resistances are divided into two equal parts and soldered on both sides of the substrate. The distributions of characteristic impedances and isolation resistances can be obtained by searching tables [28], as listed in Table 1.

D. OPTIMUM DESIGN AND PERFORMANCE

To evaluate the performance of the proposed balun, we also use ANSYS HFSS 2018 to carry out some simulations, and the structural configuration of the balun is depicted in Fig. 7. For this design, a RT5880 substrate with dielectric constant of 2.2 and thickness of 1.57 mm is also adopted. Due to engineering constraints, the closest to the halves of the isolation resistances available in market are $R_1 = 51$ ohms and $R_2 = 120$ ohms. Therefore, some parameters are optimized for good performance, which are (unit: mm): $w_1' = 4$, $w_2' = 5.7, w_5 = 3.1, w_6 = 4, w_7 = 3.8, w_8 = 19.48, l_2' = 3, l_7 = 2.7, l_8 = 3, l_9 = 0.5, r_2 = 14.7, r_3 = 5.4, r_4 = 7.1, r_5 = 6.1, r_6 = 3$ (The same parameters mentioned above are not repeated here). The corresponding fabrication is depicted in Fig. 8, and the measurements are carried out in the form of two-port test, as shown in Fig. 9.

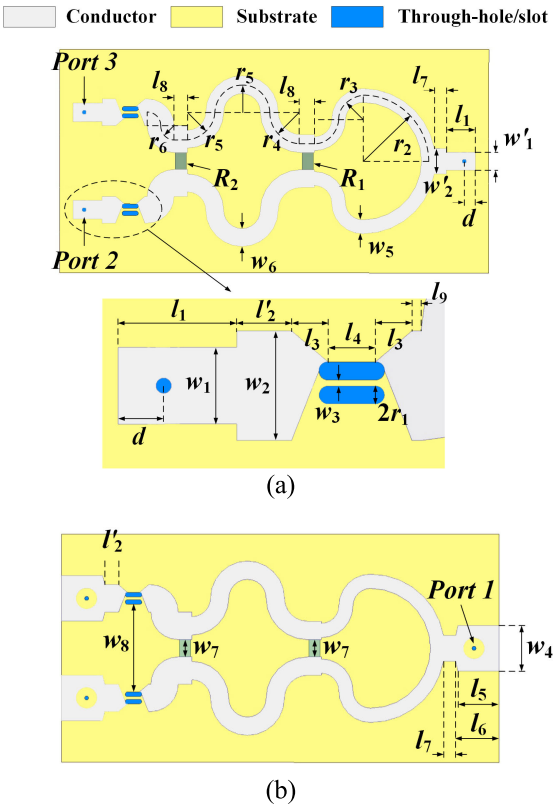

FIGURE 7. Structural configuration of the balun. (a) Top view. (b) Bottom view.

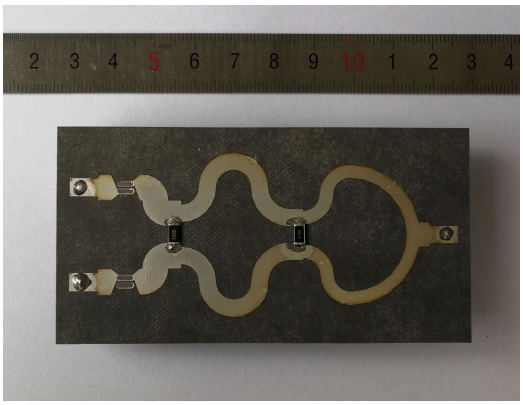

FIGURE 8. Fabrication of the balun.

From the results, we can see that in the 0.52-2.32 GHz band, the measurements can achieve the reflection, amplitude imbalance and phase imbalance characteristics below −15 dB, ±0.46 dB and ±4 deg, respectively. In addition, the isolation of two balanced ports is larger than 15dB in the working band. Due to the similar reasons listed in part B, the measured results are worse than those obtained by simulation. However, from their similar trends, we can conclude that the measurements still have good agreement with the simulations. Table 2 lists a comparison of the measurements carried out in this work and other baluns, from which we can see that the given balun is competitive in performance.

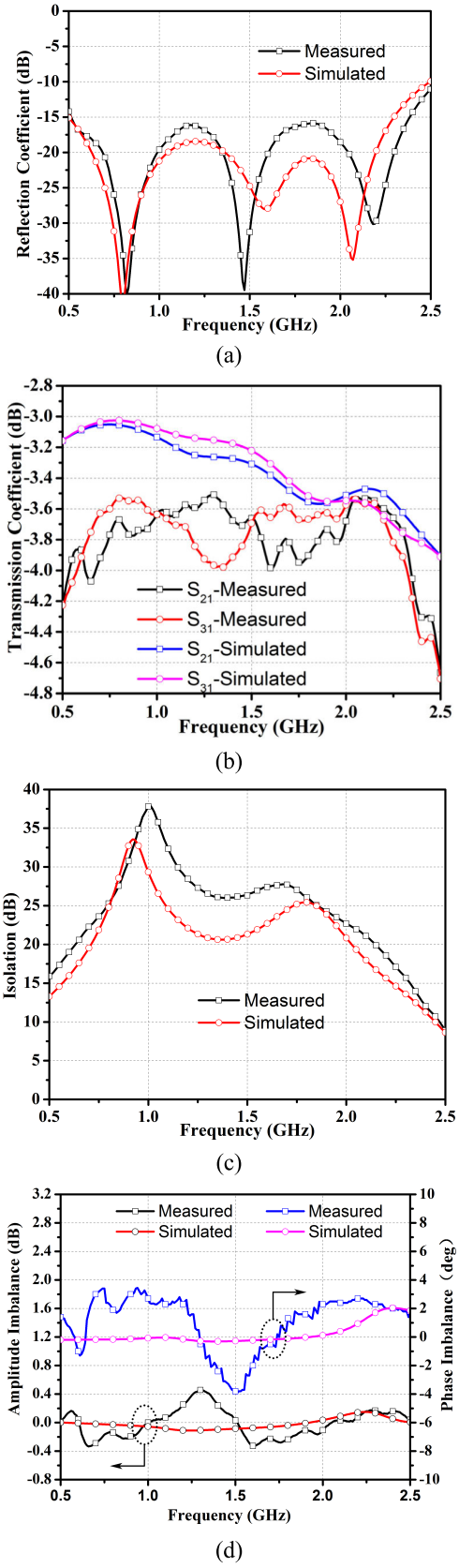

FIGURE 9. The Comparison of simulations and measurements of the experiment. (a) Reflection coefficient. (b) Transmission coefficients. (c) Isolation. (d) Amplitude imbalance and phase difference.

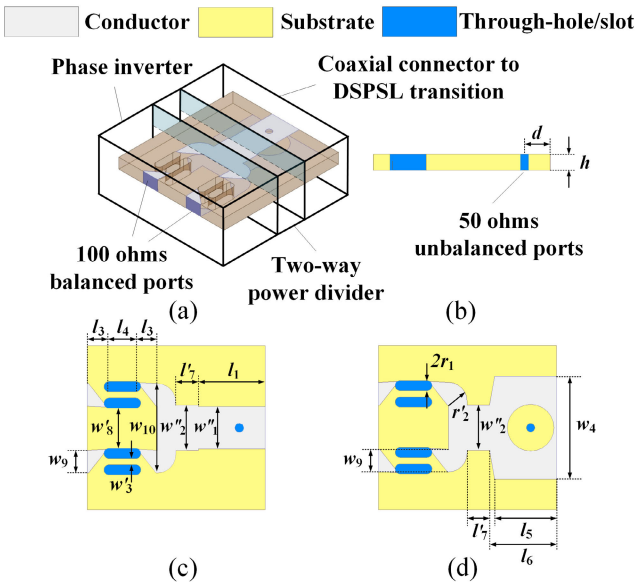

FIGURE 10. Structural configuration of the 1:2 balun. (a) Top view. (b) Overall view. (c) Bottom view. (d) Side view.

III. POTENTIAL EXPLORATION OF THE BALUN

As is known to all, the working bandwidth of multi-section impedance depends on the number of sections. Considering that the impedance bandwidth of the proposed balun is mainly limited by the two-section impedance transformer, a prototype with a 1:2 impedance ratio is presented to investigate the bandwidth potential of the 1:1 balun presented in section II. The structural configuration of the 1:2 balun is depicted in Fig. 10, which is composed of a coaxial connector to DSPSL transition, a two-way power divider, and a phase inverter.

First, we can simply study the performance of the 1:2 balun by analyzing the reflection contribution of each part to the total reflection. For instance, the similar transmission modes and nearly 50 ohms characteristic impedances of the coaxial connector and the DSPSL can lead to little reflection in the wideband for the coaxial connector to DSPSL transition. For the two-way power divider, the parallel impedance of two 100-ohm outputs frequency independently matches with the 50 ohms impedance of the input. For the phase inverter, each DSPSL can be designed to be nearly 100 ohms impedance to reduce reflection. Therefore, when the impedance transformer is removed, almost all the remaining structures of the proposed balun can theoretically achieve good matching with a frequency independent characteristic.

Second, some simulations and experiments are carried out to verify the UWB performance of the 1:2 balun. The characteristic impedance of the phase inverter needs to be adjusted to 100 ohms to match each output of the two-way power divider, which can be calculated to be approximately 1mm. The distance between two ways of the divider is sub-

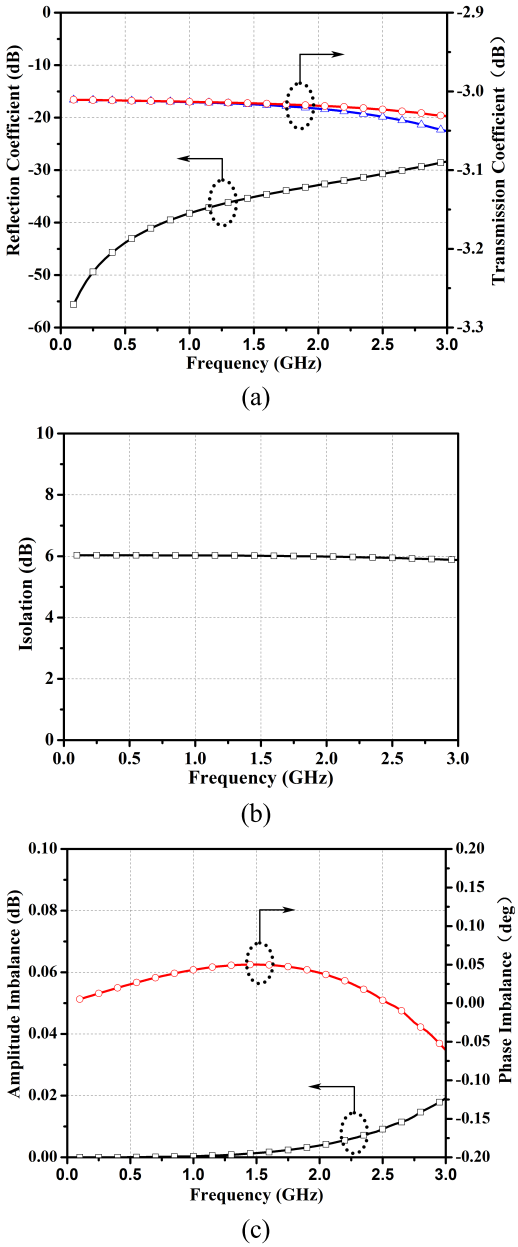

FIGURE 11. Simulations of the 1:2 balun. (a) Reflection and transmission coefficient. (b) Isolation. (c) Magnitude imbalance and phase imbalance.

stantially narrowed so that the influence of the impedance deviation of designed DSPSL and the theoretical impedance of 50 ohms can be reduced. We can simply get this conclusion from the impedance transformation formula of (5), as follows:

$$Z_{out} = Z_0 \frac{Z_{in} + jZ_0 \tan\theta}{Z_0 + jZ_{in} \tan\theta}, \tag{5}$$

where Z_{out} is the output impedance, Z_{in} is the intput impedance, Z_0 is the characteristic impedance of the transformer and θ is the electric length of the transformer.

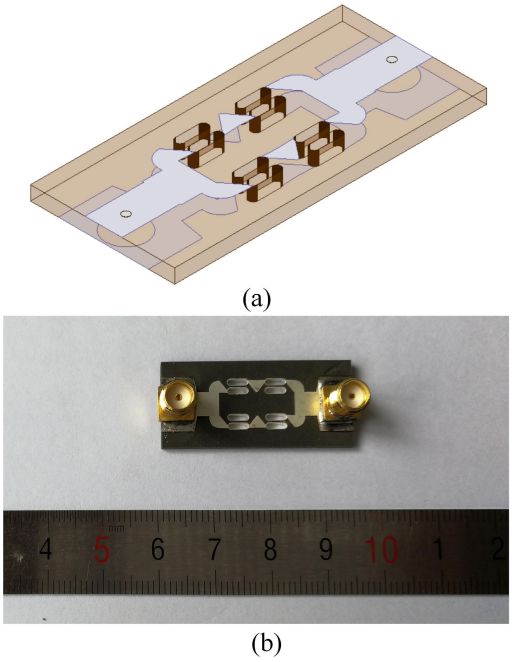

FIGURE 12. Back-to-back structure. (a) Simulation model. (b) Fabrication.

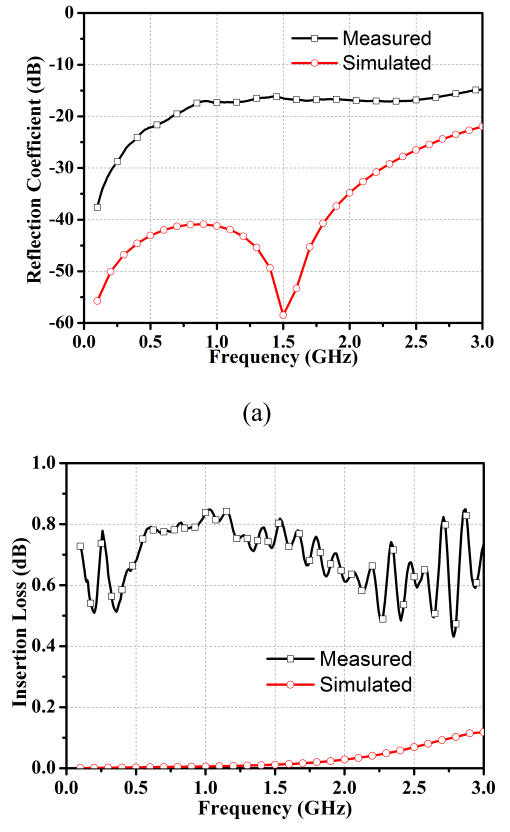

FIGURE 13. Comparison of simulations and measurements of the back-to-back structure. (a) Reflection coefficient. (b) Insertion loss.

In this design, the electric length of the transformer is less than a quarter wavelength, and by deriving (5) we can obtain

TABLE 2. Comparison between baluns.

Type	Band (GHz)	Reflection (dB)	Insertion loss (dB)	Isolation (dB)	Amplitude imbalance (dB)	Phase imbalance (deg)	Structural complexity	Ref.
Marchand	2.25-2.68	<-10	N/A	N/A	±0.19	±1.32	Simple	[4]
Coupled line	0.86-1.02 2.46-2.6	<-10	<1 <1.5	>10	±1	±5.7 ±7.95	Simple	[6]
90° phase shifter based trans. line	1-2.25	<-10	<0.8	N/A	±1	±3.4	Complex	[18]
Coupling slot based trans. line	46.7-74.8	<-10	<2.5	N/A	±0.4	±5	Medium	[22]
Conductor exchange based trans. line	1.6-10	<-10	<2	>10	N/A	±5	Medium	[23]
Conductor exchange based trans. line	19-29	<-15	N/A	N/A	±1	±5	Medium	[25]
Conductor exchange based trans. line	0.52-2.32	<-15	<1	>15dB	±0.46	±4	Medium	This work

Trans. line: Transmission line; SIWR: Substrate integrated waveguide resonator;
Amplitude imbalance: $10*\lg(|S_{21}|)$-$10*\lg(|S_{31}|)$;
Phase imbalance: $\angle|S_{21}|$-$\angle|S_{31}|$-180°.

the conclusion that when $Z_0 > Z_{in}$, Z_{out} increases with $\tan\theta$, and when $Z_0 < Z_{in}$, Z_{out} decreases with $\tan\theta$. Therefore, the smaller the $\tan\theta$, the closer Z_{out} is to Z_{in}, which confirms the inference above.

The ANSYS HFSS 2018 is also utilized to calculate the 1:2 balun and optimize its parameters for obtaining good performance. The modified parameters are (unit: mm): $h = 1.57, w_1'' = 4.1, w_3'' = 0.6, w_8' = 3.9, w_9 = 2.2, w_{10} = 8.7, l_7' = 2.2, r_2' = 2.2$. The simulated results are depicted in Fig. 11.

From the simulations, we can see that the balun can achieve the reflection, amplitude imbalance and phase imbalance characteristics below −28 dB, 0.02 dB and ±0.07 deg in the 0.1 GHz to 3 GHz band, respectively. However, similar to the quarter-wave transformer, the Wilkinson isolation circuit also needs to be connected with several quarter wavelength transmission lines and multi-stage isolation resistances to expand the high isolation bandwidth. Therefore, when the multi-section part is removed from this exploration, the isolation of two outputs can only be approximately 6dB, which is the same as that for the two-way power divider.

As the 1:2 balun has an output characteristic impedance of 100 ohms, which cannot be directly measured with the VNA, a back-to-back structure is proposed to verify its reflection and insertion loss characteristics. The balun is connected to its 180-degree rotating copy to form a back-to-back structure, as depicted in Fig. 12 (a). The corresponding fabrication is shown in Fig. 12 (b), and a comparison of measurements and simulations is given in Fig. 13.

From the results, we can see that the back-to-back structure can achieve the reflection and insertion loss of below −21 dB and 0.12 dB for simulations, and −15 dB and 0.85 dB for measurements. Except for the same errors discussed in section II part B, the measurements show a good agreement with the simulations.

In this exploration, we find that the proposed balun has the potential to work in a wider frequency band. We can boldly predict that a better UWB 1:1 balun can be designed by using the Wilkinson impedance transformer with more sections when some problems that may arise are solved, such as coupling, loss, device size, resonance and so on.

In addition, the 1:2 balun also has some potential applications, such as for balanced low noise amplifiers with its input impedance higher than 50 ohms to realize noise figure improvement [29], [30] and differentially fed ridged horn antenna [31] if its input impedance is adjusted to 100 ohms for a better match in band.

IV. CONCLUSION

A planar ultra-wideband transmission line balun based on a novel phase inverter is proposed in this work. The principle of phase inversion is interpreted, and the performance of the phase inverter is analyzed, verified and discussed. Then, a brief structural introduction and performance of the balun is presented. Finally, the UWB potential of the balun is studied with a 1:2 balun design, which shows a positive validation. All of the measurements show good agreement with the corresponding simulations considering the errors introduced by unexpected resonance, dielectric constant instability and processing errors of the metalized slots. Above all, the designed balun shows the competitive performance and great potential, which is suitable to feed the differentially fed antennas or other integrated circuits.

REFERENCES

[1] H. Jia, B. Chi, L. Kuang, and Z. Wang, "A W-band power amplifier utilizing a miniaturized marchand balun combiner," *IEEE Trans. Microw. Theory Techn.*, vol. 63, no. 2, pp. 719–725, Feb. 2015.

[2] T. K. Johansen and V. Krozer, "A 38 to 44 GHz sub-harmonic balanced HBT mixer with integrated miniature spiral type Marchand balun," *Prog. Electromagn. Res.*, vol. 135, pp. 317–330, 2013.

[3] M. H. Novak and J. L. Volakis, "Ultrawideband antennas for multiband satellite communications at UHF–Ku frequencies," *IEEE Trans. Antennas Propag.*, vol. 63, no. 4, pp. 1334–1341, Apr. 2015.

[4] Y. Wang and J.-C. Lee, "A miniaturized marchand balun model with short-end and capacitive feeding," *IEEE Access*, vol. 6, pp. 26653–26659, 2018.

[5] R. K. Barik, K. V. P. Kumar, and S. S. Karthikeyan, "Design of a quad-band branch line balun using extended Pi-shaped coupled lines," *IEEE Microw. Wireless Compon. Lett.*, vol. 26, no. 10, pp. 771–773, Oct. 2016.

[6] Y. Wu, L. Yao, W. Zhang, W. Wang, and Y. Liu, "A planar dual-band coupled-line balun with impedance transformation and high isolation," *IEEE Access*, vol. 4, pp. 9689–9701, 2016.

[7] R. K. Mongia, "Baluns," in *RF and Microwave Coupled-Line Circuits*, 2nd ed. Fitchburg, MA, USA: Artech House, 2007, pp. 486–490.

[8] Y.-W. Zhong, G.-M. Yang, J.-Y. Mo, and L.-R. Zheng, "Compact circularly polarized archimedean spiral antenna for ultrawideband communication applications," *IEEE Antennas Wireless Propag. Lett.*, vol. 16, pp. 129–132, 2017.

[9] L. Chiu, T. Yum, Q. Xue, and C. Chan, "A wideband compact parallel-strip 180° Wilkinson power divider for push-pull circuitries," *IEEE Microw. Wireless Compon. Lett.*, vol. 16, no. 1, pp. 49–51, Jan. 2006.

[10] Y. Tian, H. Wang, Z. Liu, Q. Meng, and K. Lee, "Low-loss micro-coaxial rat-race hybrid for Si-based microwave integrated circuits," *IEEE Microw. Wireless Compon. Lett.*, vol. 26, no. 3, pp. 162–164, Mar. 2016.

[11] M. Mansouree and A. Yahaghi, "Planar magic-tee using substrate integrated waveguide based on mode-conversion technique," *IEEE Microw. Wireless Compon. Lett.*, vol. 26, no. 5, pp. 307–309, May 2016.

[12] Y.-L. Yao, "Planar wideband balun with novel slotline T-junction transition," *Prog. Electromagn. Res.*, vol. 64, pp. 73–79, 2016.

[13] F. Huang, J. Wang, J. Hong, and W. Wu, "Wideband balun bandpass filter with broadside-coupled microstrip/slotline resonator structure," *Electron. Lett.*, vol. 53, no. 19, pp. 1320–1321, Sep. 2017.

[14] F. Huang, J. Wang, K. Aliqab, J. Hong, and W. Wu, "Analysis and design of a new self-packaged wideband balun bandpass filter with the functionality of impedance transformation," *IEEE Trans. Microw. Theory Techn.*, vol. 67, no. 6, pp. 2322–2330, Jun. 2019.

[15] L.-P. Feng and L. Zhu, "Compact wideband filtering balun using stacked composite resonators," *IEEE Access*, vol. 6, pp. 34651–34658, 2018.

[16] J. Zhou, H. J. Qian, J. Ren, and X. Luo, "Reconfigurable wideband filtering balun with tunable dual-notched bands using CPW-to-slot transition and varactor-loaded shorted-slot," *IEEE Access*, vol. 7, pp. 36761–36771, 2019.

[17] C. Nguyen and D. Smith, "Novel miniaturised wideband baluns for MIC and MMIC applications," *Electron. Lett.*, vol. 29, no. 12, pp. 1060–1061, Jun. 1993.

[18] H.-X. Xu, G.-M. Wang, X. Chen, and T.-P. Li, "Broadband balun using fully artificial fractal-shaped composite right/left handed transmission line," *IEEE Microw. Wireless Compon. Lett.*, vol. 22, no. 1, pp. 16–18, Jan. 2012.

[19] H. Oh, W. Lee, H. Lee, H. Koo, S. Oh, K. C. Hwang, K.-Y. Lee, C.-S. Park, and Y. Yang, "A better balun? Done the design of a 4: 1 wideband balun using a parallel-connected transmission-line balun," *IEEE Microw. Mag.*, vol. 18, no. 1, pp. 85–90, Jan./Feb. 2016.

[20] P. T. Nguyen, S. Crozier, and A. Abbosh, "Wideband and compact quasi-Yagi antenna integrated with balun of microstrip to slotline transitions," *Electron. Lett.*, vol. 49, no. 2, pp. 88–89, Jan. 2013.

[21] L. Yang, W.-W. Choi, and K.-W. Tam, "Compact ultra-wideband balun filter and its quasi-Yagi antenna application," in *Proc. ISAP*, Hobart, TAS, Australia, Nov. 2015, pp. 1–3.

[22] T. Zhang, L. Li, Z. Zhu, and T. J. Cui, "A broadband planar balun using aperture-coupled microstrip-to-SIW transition," *IEEE Microw. Wireless Compon. Lett.*, vol. 29, no. 8, pp. 532–534, Aug. 2019.

[23] M. S. Mahani and R. Abhari, "A planar ultra wide band single layer microstrip BALUN operating from 200 MHz to 10 GHz," in *IEEE MTT-S Int. Microw. Symp. Dig.*, Montreal, QC, Canada, Jun. 2012, pp. 1–3.

[24] S. Sengele, "An ultra wideband, 1–20 GHz balun in an electrically small conducting enclosure," in *Proc. IEEE Int. Symp. Antennas Propag. USNC/URSI Nat. Radio Sci. Meeting*, Vancouver, BC, Canada, Jul. 2015, pp. 1390–1391.

[25] Z.-Y. Zhang and K. Wu, "A broadband substrate integrated waveguide (SIW) planar balun," *IEEE Microw. Wireless Compon. Lett.*, vol. 17, no. 12, pp. 843–845, Dec. 2007.

[26] J.-X. Chen, C.-H.-K. Chin, and Q. Xue, "Double-sided parallel-strip line with an inserted conductor plane and its applications," *IEEE Trans. Microw. Theory Techn.*, vol. 55, no. 9, pp. 1899–1904, Sep. 2007.

[27] T. C. Edwards and M. B. Steer, "Microstrip design at low frequencies," in *Foundations for Microstrip Circuit Design*, 4th ed. Hoboken, NJ, USA: Wiley, 2016, pp. 147–148.

[28] S. B. Cohn, "A class of broadband 3-port TEM hybrids," *IEEE Trans. Microw. Theory Techn.*, vol. MTT-16, no. 2, pp. 110–118, Feb. 1968.

[29] L. Belostotski and J. W. Haslett, "Sub-0.2 dB noise figure wideband room-temperature CMOS LNA with non-50 Ω signal-source impedance," *IEEE J. Solid-State Circuits*, vol. 42, no. 11, pp. 2492–2502, Oct. 2007.

[30] T. Chong, "A low-noise, high-linearity balanced amplifier in enhancement-mode GaAs pHEMT technology for wireless base-stations," in *Proc. Eur. Gallium Arsenide Other Semiconductor Appl. Symp.*, Paris, France, May 2006, pp. 461–464.

[31] T. S. Beukman, "A quadraxial feed for ultra-wide bandwidth quadruple-ridged flared horn antennas," in *Proc. 8th EuCAP*, The Hague, The Netherlands, Apr. 2014, pp. 1149–1152.

YA-QING YU was born in Zhejiang, China, in October 1990. He received the B.S. degree in electromagnetic field and wireless technology from Xidian University, Xi'an, China, in 2013, where he is currently pursuing the Ph.D. degree in electromagnetic field and microwave technology.

His research interests include wideband antennas, wide beam antenna, and antenna feeding structure.

WEN JIANG (Member, IEEE) was born in Shandong, China, in November 1985. He received the B.S. and Ph.D. degrees from Xidian University, Xi'an, China, in 2008 and 2012, respectively.

He is currently the Vice Director of the National Key Laboratory of Science and Technology on Antennas and Microwaves, Xidian University, where he is also an Associate Professor. His current research interests include electromagnetic scattering and stealth technology, antenna theory and engineering, and electromagnetic measurement theory and technology.

LV QIN was born in Guangxi, China, in 1979. He received the bachelor's degree in computer communications from the College of Electronic Information, Sichuan University.

He is currently a Senior Engineer with the 39th Research Institute of China Electronics Technology Group Corporation. He has presided over or participated in many 863 and 973 National Key Research and Development Projects about the design of feed systems, such as high-power measurement radar, TT&C antenna, and radio telescope antenna. His current research interests include the design of horn antenna, feed antenna, and components of the feed.

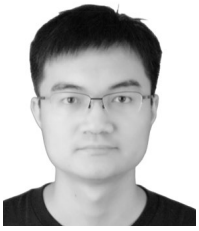

HAO-YU SHAO was born in Sichuan, China, in 1991. He received the B.S. degree in electronic information science and technology from Xidian University, Xi'an, China, in 2014, where he is currently pursuing the Ph.D. degree.

His research interests include antenna design and antenna array optimization.

SHU-XI GONG (Member, IEEE) was born in Hebei, China, in March 1957. He received the B.S. and M.S. degrees from Xidian University, Xi'an, China, in 1982 and 1984, respectively, and the Ph.D. degree from Xi'an Jiaotong University, Xi'an, in 1988.

He was the Director of the National Key Laboratory of Science and Technology on Antennas and Microwaves, Xidian University, where he is currently a Full Professor. He has authored or coauthored over 200 refereed journal articles. He has also authored Principles of *Generalized Eigenfunction Expansions in Electromagnetic Theory* (Xi'an: Xidian University Press, 2010), *Prediction and Reduction of Antenna Radar Cross Section* (Xi'an: Xidian University Press, 2010), and *Antennas for Mobile Communication Systems* (Beijing: Electronics Industry Press, 2011). His current research interests include antenna theory and technology, prediction and control of antenna radar cross section (RCS), and RCS calculation of complex targets.

Dr. Gong is a Senior Member of the Chinese Institute of Electronics (CIE) and the Vice Chairman of the Antenna Society of CIE. He is an Editorial Board Member of the Chinese *Journal of Xidian University* and the *Journal of Microwaves*. He was a recipient of the Science and Technology Advancement Award of Shaanxi Province, the Science and Technology Advancement Award of the Ministry of Information Industry of China, the Yilida Best Paper Award of Chinese *Journal of Radio Science*, the Outstanding Young Scholar Award of the Ministry of Mechanical Electronics of China, and the Excellent Young Backbone Teacher Award of the National Education Committee of China.